Filter function of graphene oxide: Trapping perfluorinated molecules

The Journal of Chemical Physics

Filter function of graphene oxide: Trapping perfluorinated molecules

Cite as: J. Chem. Phys. **152**, 024704 (2020); https://doi.org/10.1063/1.5132751
Submitted: 18 October 2019 . Accepted: 18 December 2019 . Published Online: 09 January 2020

David Barker, Angelica Fors, Emelie Lindgren, Axel Olesund, and Elsebeth Schröder

The Journal of Chemical Physics ARTICLE scitation.org/journal/jcp

Filter function of graphene oxide: Trapping perfluorinated molecules

Cite as: J. Chem. Phys. 152, 024704 (2020); doi: 10.1063/1.5132751
Submitted: 18 October 2019 • Accepted: 18 December 2019 •
Published Online: 9 January 2020

David Barker,[a),b)] Angelica Fors,[a)] Emelie Lindgren,[a)] Axel Olesund,[a),c)] and Elsebeth Schröder[d)]

AFFILIATIONS

Microtechnology and Nanoscience, MC2, Chalmers University of Technology, SE-412 96 Göteborg, Sweden

[a)]**Contributions:** D. Barker, A. Fors, E. Lindgren, and A. Olesund contributed equally to this work.
[b)]**Present address:** NanoLund and Solid State Physics, Lund University, SE-221 00 Lund, Sweden.
[c)]**Present address:** Chemistry and Chemical Engineering, Chalmers University of Technology, SE-412 96 Göteborg, Sweden.
[d)]**Electronic mail:** schroder@chalmers.se

ABSTRACT

We need clean drinking water, but current water purification methods are not always sufficient. This study examines the binding and binding mechanisms when graphene oxide is used as a filter material for removing perfluorinated substances and trihalomethanes. We use density functional theory calculations to examine the binding of the harmful molecules on graphene oxide. Our results indicate that the binding energies between graphene oxide and the investigated molecules are in the range of 370–1450 meV per molecule, similar to the binding energies obtained in other studies, where adsorption of similar size molecules onto graphene oxide has been investigated. This indicates that graphene oxide has the potential to separate the molecules of interest from the water. Significant contribution to the binding energies comes from the van der Waals (dispersion) interaction between the molecule and graphene oxide, while the hydrogen bonding between the functional groups of graphene oxide and the hydrogen atoms in functional groups on the molecules also plays a role in the binding.

I. INTRODUCTION

Access to clean water is essential for humanity but is presently not available to everyone. A significant amount of water sources contain bacteria and/or pollutants. Every year, 1.7×10^6 people die of various diseases caused by dirty water,[1] and 750×10^6 people currently lack access to clean drinking water.[2] Bacteria, such as *Escherichia coli* that causes diarrhea, are a major cause of diseases.[1] To remove bacteria from water, most cleaning processes add chlorine or ozone. Chlorination is effective against bacteria, but the process forms unwanted byproducts, such as harmful trihalomethanes (THM).[3]

Perfluorinated compounds (PFCs) are another group of hazardous chemicals found in water. PFCs are generally used as impregnating agents, for efficient fire fighting foam, and for creating grease-, water-, and dirt-repellent surfaces. In PFCs, the C-bonded H atoms are replaced by F atoms, and due to the strong C–F bonds,[4] the PFCs are very persistent molecules.

Even if we stopped all production and use of PFCs today, we would still have to deal with the remnants from the past 70 years of production that have polluted the environment.

Together with THM, the PFCs are examples of unhealthy substances that can be found worldwide in drinking water delivered to households,[5] also in countries where tap water is usually considered "clean," such as in Sweden.[6]

Filtering the water before sending it on to the consumer is one way to avoid the hazards of the pollutants. The molecules must be stopped by the filter, and understanding how filter materials interact with the pollutants is a step to further understand and improve the effect of filters. Popular filters consist of activated carbon, which is graphite or graphenelike, but with defects and functional groups. In an environment with water, graphene is likely to oxidize into graphene oxide (GO), with mainly two types of functional groups, the epoxide (–O–) and the hydroxyl (–OH) groups. Thus, GO is a good candidate for modeling such filters.

The purpose of this study is to use density functional theory (DFT) calculations to determine the binding of a number of THM and PFC molecules to GO and to estimate the potential of GO for use in filters for drinking water, regarding these molecules. Here, we use the vdW-DF-cx[7] version of the van der Waals density functional[8–12] (vdW-DF) method. This is done to include the long-ranged dispersion interactions in regular parameter-free DFT, crucial for physisorption. We find the adsorption energy and the structure (positions of atoms) of the THMs and PFCs when they are adsorbed on GO.

We have previously investigated the adsorption of other molecules on graphene using functionals of the vdW-DF family. Examples are benzene and naphthalene,[13] phenol,[14] adenine[15] and the other nucleobases,[16] chloroform and other trihalomethanes,[17] methanol,[18] methylbenzenes,[19,20] n-alkanes,[21] and, more recently, chloroform adsorbed on GO.[22] These and similar results all provide fundamental knowledge on the molecular-level binding properties in carbon-based filters.

The outline of this paper is as follows: In Sec. II, we describe graphene oxide and the adsorbed molecules of this study: perfluorinated molecules and trihalomethanes. Section III describes the method of computation, Sec. IV reports the results of our calculations and discusses them, and in Sec. V, we summarize the study.

II. MATERIALS

Our material of focus in this study is carbon-based filters and members of two different groups of pollutants, the small THMs and the polymeric PFCs.

A. Pollutants and filters

THMs are methanelike molecules in which three of the four H atoms are substituted by halogen atoms, such as Cl, Br, or F. Several THMs are formed as byproducts from disinfection of water using halogens,[23] such as in chlorination. Because this type of purification is used by many treatment plants, THM occurs in almost all tap water. The most common THM formed in the purification process is chloroform, $CHCl_3$, but also Br-containing THMs are formed. THM has shown several adverse health effects, including risk of tumors in kidney, liver, and colon. It is also suspected that high doses of THMs affect reproduction.[24,25]

PFCs are polymers in which all C–H bonds are replaced by C–F bonds. PFCs pose various serious health risks.[6] PFCs have been produced since 1950, and they are long-lived, as the C–F bonds are not broken down naturally. An example of everyday use of PFCs is as a dirt-repellent in the textile industry.[26] Laundering of textiles treated with PFC causes these substances to spread further in the water system.[27] The PFCs spread easily over long distances, via water currents and in the atmosphere, and once they enter a water environment, they are difficult to remove by conventional water filtering methods.[28–31]

A conventional way to clean water is to let it sift through a filter bed of activated carbon. This is still the most efficient method to remove PFC, but the filter material needs to be changed frequently.[32,33] Activated carbon has a high surface area to volume ratio due to the small voids and pores in the graphitic material. The effectiveness of such filters for THMs and PFCs depends on the size and composition of the pollutant, where large molecules in general are more easily retained in the filter. Once the pollutants fill the filter, one can either flush the pollutants back out and deal with the fluid of concentrated pollutants by other means, or burn the filter, including the pollutants, at very high temperatures.

Here, we use partly oxidized GO as a model for activated carbon filters. Graphene is a single layer of graphite and can be produced by a number of different methods: some methods produce high-quality graphene, and others are better suited for large-scale production. Once subjected to water, as in the water filters, graphene oxidizes and eventually becomes GO, if not already partly oxidized in the production process. For studies of carbon-based water filters, GO is therefore a better model than pristine (i.e., clean) graphene.

B. Graphene oxide

In GO, or partly oxidized graphene, the functional groups are not distributed in any systematic manner.[22,34] This means that the distribution of O across GO, in epoxide or hydroxyl groups, is more or less random. In real GO, there are carboxyl groups present at the edges of GO. In this study, we use periodically repeated GO (i.e., in principle an infinite sheet of GO), which has no edges, and thus, carboxyl groups are less relevant here.

In the epoxide group, the O binds to two neighboring graphene C atoms, whereas in hydroxyl, the O binds to one graphene C atom and one H atom. The C–O–C angle in the epoxide groups is different from the angle in usual C–O–C bindings and the bonds are therefore relatively easy to break, making the epoxide groups reactive. In the present study, however, we focus on molecules that physisorb on GO, i.e., the process does not break any covalent bonds in GO.

One frequently used model of GO proposed by Lerf *et al.*[34] is based on GO created by chemical processes. For the present study, a variant of the Lerf model was constructed, illustrated in Fig. 1. As in the original Lerf model, the GO is not fully oxidized, the functional groups are more concentrated in some parts of the graphene sheet, and the distribution of functional groups between the two sides of graphene is not entirely even. This results in a slight bending of the carbon plane of GO (see Fig. 1). Our GO model contains, per unit cell, nine epoxide and seven hydroxyl groups, along with 100 C atoms. The epoxide groups are in the majority (in our model and in the Lerf model) because their binding energy to graphene is significantly higher (more favorable for binding) than the binding energy of the hydroxyl groups.[22,35]

We focus on investigating the physisorption of a number of molecules on GO, and by using one and the same model for GO in all our calculations (Fig. 1), we can more easily compare how changes in the molecules affect the results.

C. Trihalomethanes

We here consider two THMs: chloroform ($CHCl_3$) and bromodichloromethane ($CHBrCl_2$). Their structures are shown in the two top panels of Fig. 2. Chloroform adsorption on GO, which had a different distribution of functional groups, was also studied in a previous work by one of us, using the same computational method.[22]

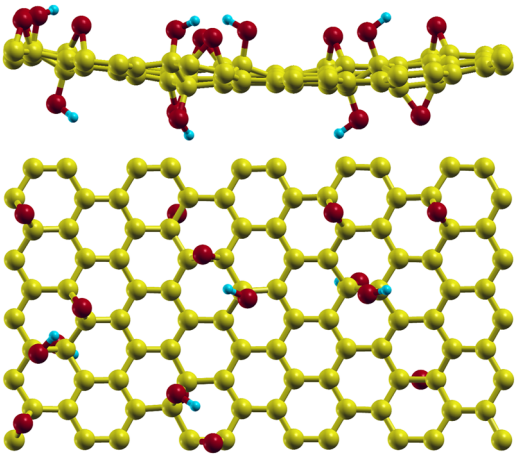

FIG. 1. One unit cell of the graphene oxide (GO) model chosen in this work. It includes nine epoxide groups (–O–) and seven hydroxyl groups (–OH) per 100 C atoms, distributed on both sides of the sheet, which is about 1/3 of fully saturated GO with the approximate formula $C_8O_2(OH)_2$. Note the slight bending of the graphene plane, due to the uneven distribution of functional groups. The color coding of the atoms is C-yellow, H-blue, and O-dark red.

D. Perfluorinated compounds

Four PFCs have been selected for the present study, and their structures are presented in Fig. 2. These are perfluorooctanoic acid (PFOA, $C_8HF_{15}O_2$), perfluorobutane sulfonic acid (PFBS, $C_4HF_9O_3S$), perfluorohexane sulfonic acid (PFHxS, $C_6HF_{13}O_3S$), and perfluorooctane sulfonic acid (PFOS, $C_8HF_{17}O_3S$). The last three sulfonic acids contain a sulfonyl hydroxide ($-SO_3H$) group in one end, and here we order them in increasing length of the C backbone.

The four PFC molecules share similarities: PFOA contains O and OH functional groups in one end, whereas the similarly sized (same number of CF bonds) PFOS instead contains a SO_3H group. PFBS and PFHxS, like PFOS, contain the SO_3H group but have shorter C backbones (and thus fewer CF bonds).

III. METHOD OF COMPUTATION

For the DFT calculations, we use the vdW-DF method[7–12] in which the exchange-correlation approximation includes long-range dispersion interactions. We use the consistent-exchange version vdW-DF-cx[7] that is highly accurate in the description of many different types of systems, also when interactions compete.[11,36–44] We use the DFT code Quantum Espresso (QE)[45,46] with a fast-Fourier-transform implementation of the central integral in the nonlocal correlation calculations.[47]

All calculations are carried out using periodically repeated orthorhombic unit cells. Each unit cell contains 100 C atoms of GO, the GO functional groups, and the adsorbed molecule. The size of the unit cell is 21.3 Å × 12.3 Å in the plane of GO, and usually 15.0 Å in the perpendicular direction. For the case when PFOA is "standing up" on GO, the size in the perpendicular direction is increased to 21.3 Å. The unit cell with one unit of GO is illustrated in Fig. 1.

We use a 2 × 2 × 1 k-point Monkhorst-Pack (MP) sampling over the Brillouin zone (BZ).[48] The atomic positions are optimized by minimizing the forces acting on them, and the atomic positions are considered relaxed when all components of all forces are smaller than $3 \cdot 10^{-4}$ a.u. (≈0.015 eV/Å), which is 30% of the QE default value. We use ultrasoft Perdew-Burke-Ernzerhof[49] (PBE) pseudopotentials from the GBRV package[50] and their recommended wave function (electron density) energy cutoff values 40 Ry (200 Ry). Energy convergence for each atomic configuration is obtained when the total energy changes less than 10^{-8} Ry per iteration, or approximately 10^{-7} eV.

The adsorption energy E_a is defined as the gain in total energy of a molecule adsorbed on GO, compared to the sum of total energies of isolated GO and the isolated molecule, in all calculations using the same periodic unit cell. When molecules bind on GO, we define E_a to have a positive value.

Each calculation of a molecule (PFC or THM) adsorbed on GO is started with the molecule in a number of predefined positions and orientations. The PFC molecules are initially positioned such that the plane of the C backbone is parallel with the GO plane. All PFC molecules are placed in approximately the same position above the GO sheet (being of different lengths, the positions of the PFCs are not identical), so as to be able to interact with

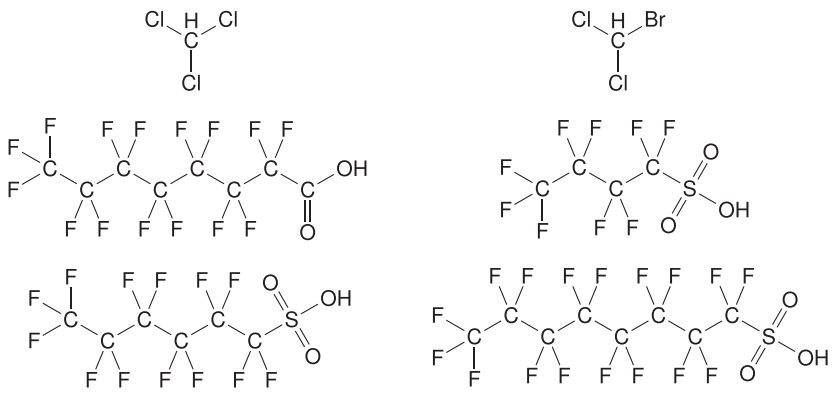

FIG. 2. The atomic structure of the trihalomethanes (top panels) and perfluorinated molecules (other four panels) considered in this work. The molecules are, left to right, top to bottom: chloroform ($CHCl_3$), bromodichloromethane ($CHBrCl_2$), perfluorooctanoic acid (PFOA, $C_8HF_{15}O_2$), perfluorobutane sulfonic acid (PFBS, $C_4HF_9O_3S$), perfluorohexane sulfonic acid (PFHxS, $C_6HF_{13}O_3S$), and perfluorooctane sulfonic acid (PFOS, $C_8HF_{17}O_3S$).

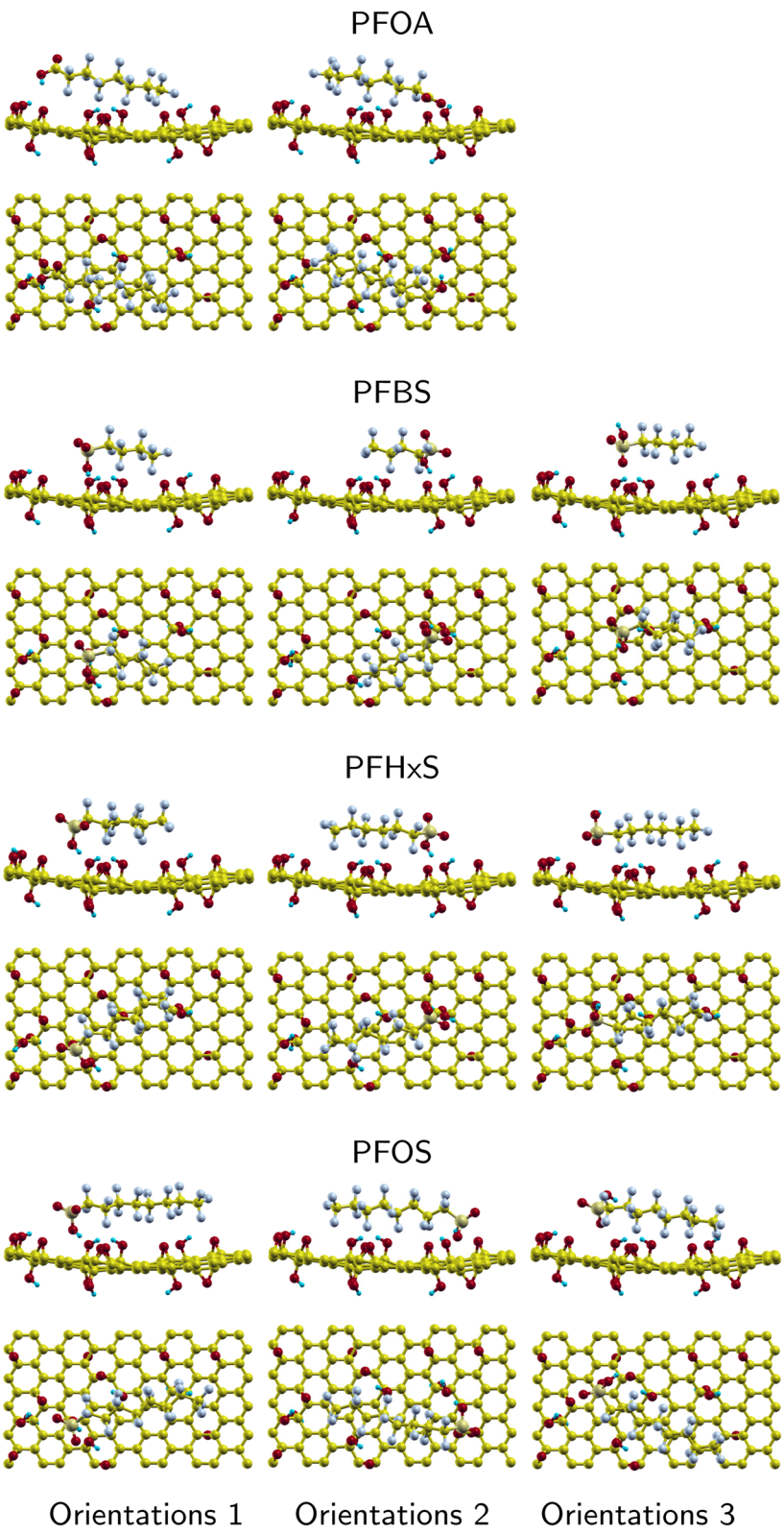

FIG. 3. Orientations of the PFCs on GO, side and top view, with optimized atomic positions. Color coding is the same as in Fig. 1 and F-light blue and S-light green.

approximately the same functional groups of GO.[51] During the calculations, some of the molecules move on GO, somewhat away from the starting position. The PFC molecule can be rotated such that the acid end of the PFC points in one or the other direction. The sulfur-containing molecules (PFBS, PFHxS, and PFOS) have an OH group (on S) pointing out of the plane of the C backbone and thus can be further oriented with this H atom pointing either toward (symbol H ↓) or away from (H ↑) the GO sheet. We calculate three of the four such possible orientations of the S-containing PFCs. On PFOA, the OH group initially lies in the plane of the backbone, and an initial "H ↓" or "H ↑" orientation cannot be assigned; there we evaluate the two possible orientations. All the (relaxed) PFC structures are illustrated in Fig. 3.

In THM adsorption, the possible orientations are less different, and we only distinguish between the H atom of the THM pointing up or down toward GO. In all cases, the THM is started in the same vicinity on GO, close to both epoxide and hydroxyl groups. The (relaxed) structures are illustrated in Fig. 4.

IV. RESULTS AND DISCUSSIONS

Our aim is to evaluate how strongly the PFC and THM molecules bind to GO in the absence of other molecules and to understand the effect on the binding of the positions and orientation of the molecules with respect to the functional groups on GO. Part of the binding energy will be due to the size of the molecule when lying flat on the GO surface (the vdW interactions), and other parts will be more specific to the interaction of the molecule and GO functional groups. To estimate the size effect, we used various lengths of the PFC molecules, and for studying the interaction of functional groups, we also carried out calculations for the PFC and THM molecules on graphene, all in approximately the same initial configurations as on GO.

Since GO has functional groups that are unevenly distributed, it is not possible to systematically survey all possible positions and orientations of the molecules relative to GO. Instead, we report the results from a few representative configurations. In all but one case, we have oriented the PFC molecule parallel to GO because we expect

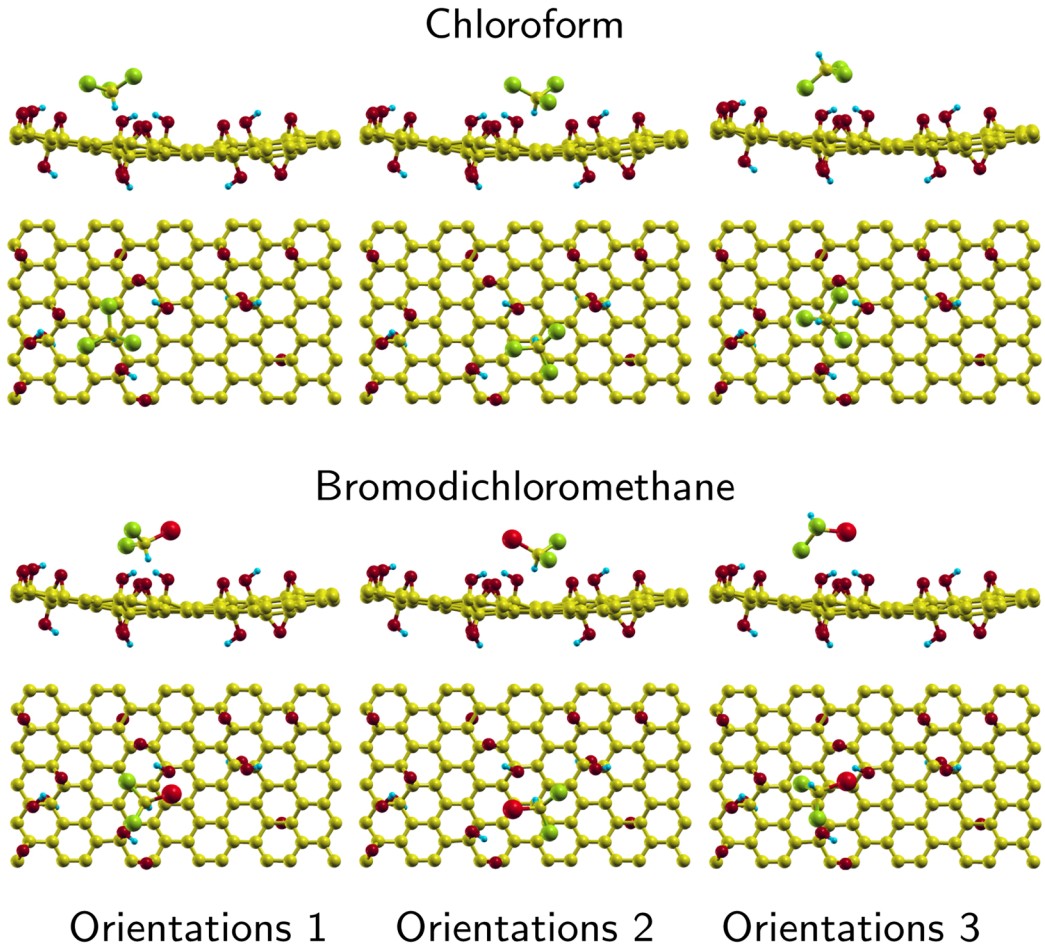

FIG. 4. Orientations of the THMs on GO, side and top view, including their naming ("Orientation No.") for each column. All atomic positions have been locally optimized by minimizing the remaining forces on the atoms. Color coding is the same as in Fig. 1, and Cl-light green and Br-lighter red.

the larger area of proximity to GO to be favorable for binding. However, for PFOA, we also carried out one calculation with PFOA perpendicular to GO, with its OH group toward GO. The THM molecules are adsorbed with the H-atom toward or away from GO, in two slightly different environments on GO.

Our study provides adsorption energies on GO, given in Table I, after local optimization of atomic positions, as illustrated in Figs. 4 and 3. For comparison, we also calculated the adsorption energies of the four PFCs and the two THMs adsorbed on graphene.

We see from Table I that the THM molecules adsorb on GO with an energy around 0.5 eV, while the PFC molecules adsorb with energies roughly in the range 0.5–1.5 eV on GO, and in the range 0.6–1.2 eV on graphene, taking all studied orientations into account. Overall, larger molecules on GO and graphene adsorb with larger energies. We discuss this in Sec. IV A. It is clear from the table that on GO, there is some variation in energy concerning the presence, orientation, and position of functional groups on the molecules, and their positions relative to the GO functional groups. The effect of this is discussed in Secs. IV B and IV C.

TABLE I. Adsorption energies E_a on GO and graphene (Gr) for the THM and PFC molecules included in this study. For the definition of orientation numbers, refer to Figs. 3 and 4. Also noted is whether the methyl group of the adsorbant has the H atom pointing toward GO (H ↓) or away from GO (H ↑), where relevant. For each molecule, an average adsorption energy is also given, as discussed in the text. Entries in italics are not included in the averages. All energies are in units of meV/molecule.

Adsorbant	Orientation	On GO	On gr
Chloroform	Orient. 1 (H ↓)	519	428
	Orient. 2 (H ↓)	544	
	Orient. 3 (H ↑)	378	417
	Average	480	
Bromodichloro-methane	Orient. 1 (H ↓)	403	447
	Orient. 2 (H ↓)	561	
	Orient. 3 (H ↑)	371	437
	Average	447	
PFOA	Orient. 1	982	1031
	Orient. 2	1208	1032
	Upright	*787*	
	Average	1095	1032
PFBS	Orient. 1 (H ↓)	1062	674
	Orient. 2 (H ↓)	1039	735
	Orient. 3 (H ↑)	456	641
	Average	852	683
PFHxS	Orient. 1 (H ↓)	991	945
	Orient. 2 (H ↓)	1175	977
	Orient. 3 (H ↑)	651	863
	Average	939	928
PFOS	Orient. 1 (H ↓)	1214	1135
	Orient. 2 (H ↓)	1451	1139
	Orient. 3 (H ↑)	1071	1021
	Average	1245	1098

A. Dependence on molecular size

Starting with PFC adsorption on graphene, we see that the average adsorption energy increases with molecular size, from 683 meV (for PFBS) to 1098 meV (for PFOS). The difference between PFBS and PFOS is the addition of four CF_2 units, and thus, the added energy per CF_2 unit on graphene is 104 meV. In comparison, in a study[21] using an earlier, less binding version[8] of vdW-DF, one of us found that the CH_2-units in n-alkanes bind to graphene with 75 meV/CH_2-unit.

For particular orientations, the energy change for increasing molecule size differs somewhat from the average 104 meV/CF_2-unit (95 meV/CF_2-unit for orientation 3 and 115 meV/CF_2-unit for orientation 1), which is in part due to the changing position of the sulfonyl hydroxide group with respect to the graphene honeycomb structure. This will be discussed in Sec. IV C.

The increase in adsorption energy for increasing molecular size in physisorption is not surprising: the area of graphene exposed to the molecules (that are parallel to the plane of graphene) increases and thus also the area involved in the vdW interactions between the molecule and graphene.

On GO, we also find that the adsorption energy increases as the length of the C-chain increases, from PFBS over PFHxS to PFOS.[52] Here, the difference is 852 meV (average of PFBS) to 1245 meV (PFOS), where 4 CF_2-units are added, i.e., 98 meV per CF_2 unit, but with more scattering in the numbers.

Finally, to illustrate the importance of area of proximity between the molecule and GO, we also start the PFOA molecule in an upright position, with the OH-group of PFOA pointing toward functional groups on GO (Fig. 5). We find that, despite the favorable interactions between the functional groups on PFOA and GO, the adsorption energy is 481 meV smaller than orientation 2 for PFOA, which has a similar favorable interaction of functional groups, and 195 meV smaller than the orientation 1, which does not have close interactions of functional groups. In other words, the proximity of all parts of the molecule contributes an important part to the adsorption energy. We discuss this further in Sec. IV D. We have previously shown that the overlap area is important, for example, for methylbenzenes on graphene[20] and polycyclic aromatic hydrocarbons (PAH) on graphene.[13] In the present study, we see this effect also on a surface, GO, that is much less smooth than graphene.

B. Dependence on orientation

We consider the effects on the adsorption energies of reorienting the molecule on GO. First, however, we study results of adsorption on graphene, without the GO functional groups.

For THM on graphene, we find that orientation with the H atom up (away from graphene) or down (toward graphene) differ in adsorption energy by as little as 10 meV. This should be compared to the corrugation of graphene for chloroform (the difference in adsorption energy when sliding chloroform across graphene), which is approximately 6 meV,[17] small (2%–3% of the adsorption energy)

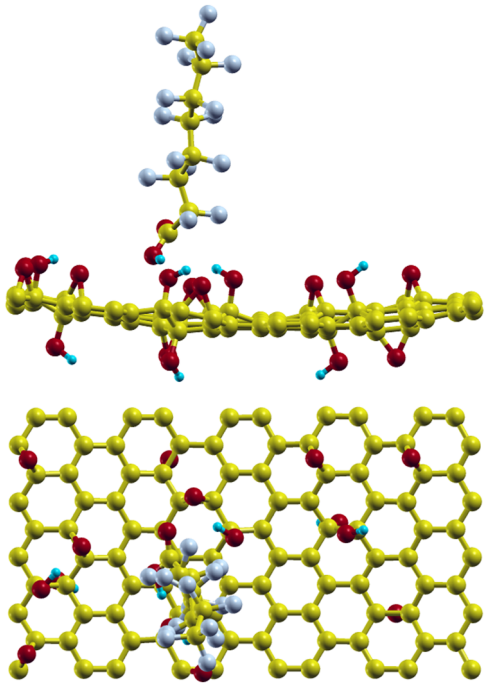

FIG. 5. PFOA, in the upright position, OH group toward GO.

and similar in size. We find that the orientation with H pointing toward graphene is slightly favorable, Table I.

One of us has previously reported results[17] on adsorption of THM on graphene, using an earlier version of vdW-DF, the vdW-DF1,[8] which generally shows less binding than the vdW-DF-cx functional choice that is used here. In that study, a slight preference for H up was found, but only at a 10 meV difference. The adsorption energies found in the previous study were 50–60 meV smaller than reported here, and the adsorption distances were 0.3 Å larger (measured as distance from THM C-atom to the plane of graphene), a result of using a functional with a more repulsive part.

For THM on GO, we also let the H-atom point either away from (up) or toward (down) the GO or graphene sheet. The THM molecules are adsorbed in two nearby areas on GO, with slightly different environments, i.e., functional groups on GO. Adsorption with H down (and consequently less of the Cl and Br atoms towards GO) is found to be favorable in the two areas of GO considered here. The energy change between the different situations on GO is larger than on clean graphene. On the average, here, we find that chloroform adsorbs on GO at 480 meV and bromodichloromethane at 450 meV, with values in the range 370–560 meV. However, as shown in Ref. 22, the preferred orientation depends strongly on the local environment on GO, such as the number, type, and positions of GO functional groups in the vicinity. In the present study, we use a larger sheet of GO for the periodically repeated GO and therefore obtain a smaller coverage of the THM and a different distribution of GO functional groups.

For PFC, we rotate the molecule such that either the OH end of PFC changes direction (from orientation 1 to orientation 2, left and middle panels of Fig. 3), or by orienting the PFC such that the OH group points away from GO (orientation 3, right panels of Fig. 3). The latter rotation is not relevant for PFOA because the initial position of the OH group is in the plane of the carbon backbone of PFOA. These three orientations then make up the small ensemble over which we determine an average adsorption energy for each of the molecules, E_{ads}^{ave} in Table I. For PFOA, we take the average over orientations 1 and 2 only.

For PFC on graphene, it is evident that the energy change with variation of orientation is small. In other words, while the detailed orientation of the PFC on the graphene honeycomb structure may play some role (comparing orientation 1, 2 and 3), it is a relatively small effect of 60 meV or less. This fits well with the previous observation[17] for the much smaller chloroform on graphene.

For PFC on GO, the orientation plays a much more important role, as does the type of functional groups involved. Table I shows that there can be more than 600 meV in adsorption energy difference for the same PFC molecule, depending on the orientation. We discuss the effect of the presence of the sulfonyl hydroxide group (in PFBS, PFHxS, and PFOS) in Sec. IV C.

C. Effect of sulfonyl hydroxide group on PFC

In the sulfonic acids PFBS, PFHxS, and PFOS, the sulfonyl hydroxide group interacts with the GO functional groups to various degrees, depending on the relative positions of the GO and PFC functional groups. Interactions between the sulfur-containing groups of PFBS, PFHxS, and PFOS, and the functional groups on GO can be studied indirectly by changing which end of the PFC has the sulfur atom. All other parts of the interaction are then approximately the same such that changes in the adsorption energy mainly arise from changes in the sulfonyl hydroxide group interaction with the functional groups of GO, near the ends of the PFC.

For example, changing the ends of PFOS (between orientation 1 and 2) gives rise to a ~ 240 meV adsorption energy difference, while for PFBS, this difference is almost nonexisting. Looking more closely at the adsorption situations (Fig. 3), we find that in orientation 1 of PFOS, the sulfur group is positioned relatively far from the GO hydroxyl groups, whereas the distance is much smaller in orientation 2 and for both of the PFBS orientations. In other words, the position of the sulfonyl hydroxide group relative to the GO functional groups is important.

Pointing the H atom of the sulfur group away from GO (orientation 3) leads to a decrease in energy of ~400–600 meV, another indication that the interaction of the sulfuric acid group with GO (and its functional groups) is important for the binding.

Now, comparing PFOS with the similarly sized (same number of C atoms) PFOA, without sulfur, we find that the adsorption energy is about 250 meV larger for PFOS, both in orientation 1 and 2, but also that the orientation of the PFOA OH group matters (energy differences of orientation 1 and 2 is ~200 meV). This is yet another indication of the importance of the sulfur group in the molecule-GO interaction, more so than the interaction of the OH group in PFOA. On the other hand, already the OH group in PFOA does make a difference in the adsorption, which we see from the energy difference ~200 meV when moving the OH group from

one end of PFOA to the other, orientation 1 to orientation 2, in other words, from one local environment to another with less functional groups on GO.

D. Changes in electron and energy density

In order to discern the mechanisms that act to bind the PFC molecules to GO, we focus on PFOS on GO, in particular, the sulfonyl hydroxide group interacting with a hydroxyl group on GO (PFOS orientation 1). As we found in Secs. IV A–IV C, both which functional groups on PFC and GO that can interact and the size of the part of the molecule that is close to GO matter for the binding strength. To improve our understanding of the origins of the binding, we analyze the changes that occur in the electron density due to the binding (Fig. 6) and the changes in the distribution of the important nonlocal exchange-correlation part of the system energy, near the molecule and GO (Fig. 7). The nonlocal exchange correlation part of the energy is mainly responsible for the vdW interactions.[8]

In our DFT calculations, we have access to the (valence) electron density, distributed in all space (the full unit cell) and represented on a dense grid. In order to see how the electron density is affected by the proximity of the two entities (PFOS and GO), we subtract from the full-system electron density the corresponding electron densities for each of the two entities, each in a unit cell of the same dimension. The atomic positions of PFOS, respectively, GO, are kept the same as in the binding situation, i.e., slightly deformed compared to their free form. The electron change that we thus obtain is then due solely to the interaction of PFOS and GO.

We find, in Fig. 6, that the only sizable change in electron density occurs where the PFOS sulfonyl hydroxide group is close to a hydroxyl group of GO, with the S–OH H-atom pointing toward the O atom of OH on GO. We see that the electron density is moved mainly into the volume exactly between the two atoms (blue isosurface), resulting in a lack of electron density on the PFOS H-atom, compared to a free PFOS molecule, but there is also a redistribution of charge internally on each of the two functional groups. It is noteworthy that there is no other redistribution of charge of this size anywhere else on PFOS or GO.

Each point in space contributes to the total energy of the combined system (in areas far from the material possibly yielding zero contribution). By subtracting the energy densities for each entity in a similar way as for the electron density, we can see where the energy contributions to the binding arise, again, ignoring for now

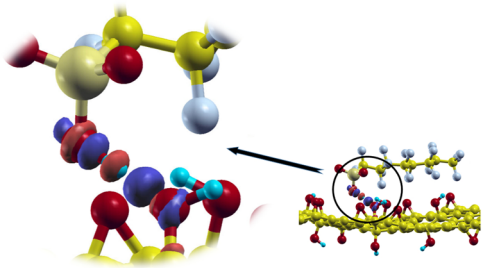

FIG. 6. PFOS— change in electron density at adsorption. Isosurfaces at $\pm 0.04 e/\text{Å}^3$, where blue is addition of electrons and red is removal of electrons.

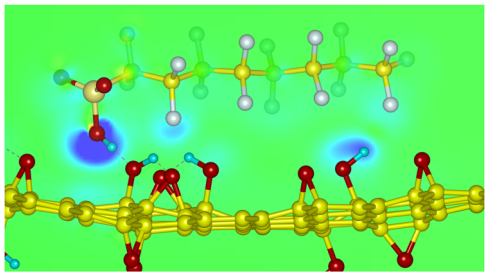

FIG. 7. PFOS— change in nonlocal exchange-correlation energy density $e_{xc}^{nl}(\mathbf{r})$ due to adsorption, shown as a cut through the PFOS molecule approximately along the C backbone, perpendicular to the GO plane. Color scale starts at -20 meV/Å^3 shown in red (only slightly visible behind the OH group of S), over zero in green, to 20 meV/Å^3 in blue. The adsorption energy is defined such that binding results in a positive (blue) energy change.

that PFOS and GO are slightly deformed when in the adsorption configuration. Since we are interested in how the vdW (dispersion) interactions affect the binding, in addition to the mutual functional-group interaction, we focus the analysis on the nonlocal part of the exchange-correlation energy density, $e_{xc}^{nl}(\mathbf{r})$. For details on the method, we referto Ref. 53.

The change in $e_{xc}^{nl}(\mathbf{r})$ is shown in Fig. 7, in a plane that cuts PFOS (approximately) through the C backbone and is perpendicular to the GO plane. Blue areas contribute to an increase in the binding energy, while red areas (hardly present in this cut) decrease it. We see that the contributions arise between the PFOS and GO, localized close to, but not on, the atoms that are closest in the binding. It is worth pointing this out because some methods for calculating the vdW interaction contribution assume an atom-centered contribution, which is not the case here, nor in general.[53,54]

We see that the $e_{xc}^{nl}(\mathbf{r})$ contributions are somewhat directional, toward atoms on the other entity. This is most clearly seen at the position of the PFOS sulfonyl hydroxide group, to the left in the plot, but contrary to the case of the electron density changes, the energy also changes at other atoms in the volume between the PFOS and GO. Summing up, the vdW interactions have contributions not only near the S–OH group but also near other positions where the PFOS and GO are at a close distance.

Hydrogen bonds consist of a collection of contributions from various mechanisms, among these electrostatic (local) exchange-correlation, and dispersive (vdW) interactions, as well as transfer of charge.[55] The latter two contributions are included in our analysis of charge (Fig. 6) and vdW interaction (Fig. 7) in the interaction region of the PFOS S–OH group. From the two figures, we interpret the interactions to consist of a hydrogen-like bond to the left on PFOS, combined with vdW interaction between all relatively close parts of the PFOS on GO.

E. Elastic and vdW energy contributions

When the molecules adsorb on GO both the molecules and GO deform, compared to their isolated structure. This is all taken care of automatically in our calculations, but for analysis, we here split the binding energy into the deformation cost and the gain of having the

two entities at adsorption distance. The deformation cost is smaller than the energy gain obtained from the interaction analyzed above (or else the system would not bind) but it lowers the binding energy.

Again, we take PFOS in orientation 1 as an example. The cost of deforming PFOS and GO, from their isolated structure to the structure in which they are found at adsorption, is calculated. For this specific example, we find the energy cost 150 meV for PFOS and 42 meV for GO, in total 192 meV. The gain of putting the deformed entities together is 1406 meV, from which the cost of deformation is subtracted to obtain binding energy 1214 meV. The elastic energy required for adsorption, 192 meV, is thus certainly smaller than the binding energy, but at 15% of the binding energy, it is not negligible and brings an important contribution to the energy balance.

To estimate the vdW interaction contribution to the binding energy, from the structures of the isolated entities to the adsorption system, we note that semilocal DFT functionals, such as PBE,[49] do not include the vdW interactions. By simply subtracting from our vdW-DF-cx calculated binding energy the PBE-based binding energy (using the vdW-DF-cx-calculated atomic positions), we obtain an estimate of the size of the vdW part of the binding. This difference, for PFOS in orientation 1, we find to be 898 meV, which is the majority of the binding energy obtained (1214 meV). We can therefore conclude that despite the H bond, which is present via the sulfonyl hydroxide group, the PFOS is attracted to GO mainly by the vdW interactions!

F. Choice of functional

In the present study, we have chosen to use the vdW-DF-cx functional for all calculations. The motivation is threefold: (i) the vdW-DF-cx is based on current conservation,[54] avoiding any fits to experimental or other benchmarking results; (ii) it has already successfully been used in a large number of adsorption studies in general, and, (iii) in particular, it is known to give results in excellent agreement with experiments for (water) adsorption on oxide surfaces.[40]

It is interesting to contrast the performance of vdW-DF-cx with another related functional that is often used in adsorption problems, the optB88-vdW functional.[56] The exchange part of this functional is based on the fitting of a parameter to the S22-benchmark set.[57] In order to compare in specific situations, we carried out adsorption calculations for two examples; the PFOS on GO in orientation 1, and chloroform on GO in orientation 2. For chloroform, the value of the adsorption energy increases from 544 meV in vdW-DF-cx to 635 meV in optB88-vdW. This is a 91 meV increase, of which only 3 meV arise from changing the atomic positions from those optimal in vdW-DF-cx to those optimal in optB88-vdW. For PFOS on GO, the value of the adsorption energy increases from 1214 meV in vdW-DF-cx to 1296 meV in optB88-vdW. In this case, the increase is 82 meV. In other words, optB88-vdW yields larger values for the adsorption energy than vdW-DF-cx, at least for these two test calculations. However, without experimental values available, we cannot determine which functional gives the most correct value.

In a preliminary study,[58] one of us revisits the desorption experiment by Zacharia *et al.*[59] of PAH molecules on graphite, an experiment that was used as the first benchmarking[13] of vdW-DF. In the new calculations, both vdW-DF-cx and optB88-vdW yield adsorption energy values that either fall within the experimental error bars or right outside. However, there also, the optB88-vdW functional yields values that are larger than for vdW-DF-cx, and they are further from the mean value of the experimental results. The tendency of optB88-vdW to slightly overestimate of the adsorption energy was also seen in Ref. 40. We therefore conclude that while optB88-vdW could be a good choice as the functional for the GO adsorption study, vdW-DF-cx is at least as good.

G. Relevance for filters

In the calculations presented here, the adsorption systems are in vacuum, which is not the situation for water or air filters. One of us has previously studied and discussed how the presence of water affects the adsorption results of, e.g., chloroform on graphene or graphene oxide.[17,22] As argued in Ref. 22, if the ground state zero-temperature adsorption energy were affected by water, seen as a continuum, that effect could only show in the part of the energy containing the nonlocal part of the correlation interaction. On the other hand, the nonlocal part of the energy is found as a sum of poles in a contour integral in the space of complex frequencies. This sum over plasmon shifts[54] starts at frequencies much higher than the range where the index of refraction for water differs from unity. This means that the presence of water does not change the nonlocal interaction.

A number of other factors also affect how pollutants bind to a filter, such as the entropy, the flow dynamics, and the molecules' solubility in water. Solubility indicates how easily molecules dissolve in water and therefore indicates the likelihood that the molecule will stay in the bulk of the water instead of binding to the filter. In the same manner, the likelihood that the pollutant molecules adsorb is also affected by the energy by which the water molecules bind to the filter, i.e., whether they fill the spot where the pollutant would otherwise adsorb. A (relatively) strong bond, combined with a high solubility of the pollutant in water, will decrease the probability of the pollutant sticking to the filter. We find the adsorption energy of a single water molecule on GO to be 594 meV and on graphene 545 meV, with the adsorption energy calculated relative to the water molecule isolated in vacuum (like for the other molecules considered here). More realistically, the water molecule would have to give up some of its bonds to the neighboring water, at a certain cost, in order to bind to GO (graphene). On GO, H_2O is placed in the most optimal environment, with one epoxide and two hydroxyl groups close by. These energies are of approximately the same size as the THM adsorption energies (slightly larger) and a factor 1.5–3 smaller than the PFC adsorption energies. Finally, when GO is used as a filter, the water will flow around the GO, causing the molecules to move and making it harder to bind to GO than if the water was not moving. These factors above are not further studied here.

V. SUMMARY

We report results on adsorption of pollutant molecules on graphene and on partly oxidized graphene, here termed GO. Two groups of pollutants are represented, the small THMs, through

chloroform ($CHCl_3$) and $CHBrCl_2$, and linear PFCs, through the molecules PFOA, PFBS, PFHxS, and PFOS.

We find that the two THMs considered here preferably adsorb with the H atom toward graphene, albeit only with a small energy difference, in size similar to the corrugation for chloroform on the smooth graphene. On GO, the energy difference is larger but depends on the local environment. The adsorption energies for the various orientations of the two THMs vary between approximately 370 meV and 560 meV on GO.

For PFCs, we find a strong preference for adsorption with the carbon backbone parallel to the plane of GO and a sensitivity to the positioning of the functional groups on the PFC and on GO relative to each other such that these are close.

For PFC, we further find that on GO, the optimal orientation (of the three studied here) has a larger adsorption energy than any of the adsorption orientations on graphene, by roughly 20%–40%. In other words, GO yields higher adsorption values, and in filters for water or air purification, this is of importance. For GO, we find that the functional groups play a decisive role in the ability to adsorb the molecules investigated. Hydrogen bonds may occur between, for example, the sulfonyl hydroxide group or F in PFC and H atoms in the hydroxyl groups of GO, indicating that a high density of hydroxyl groups at GO is advantageous for adsorption.

Finally, taking a closer look at the binding mechanisms, exemplified for PFOS in orientation 1, we find that not only the dispersion (or vdW) interactions between the elongated PFCs and GO have a major effect on the interaction but also that the H-bondlike interaction between the S–OH group on PFOS and an OH group on GO plays a role in the binding.

ACKNOWLEDGMENTS

Support from the Swedish Research Council (VR) is gratefully acknowledged. The computations were performed using resources at Chalmers Centre for Computational Science and Engineering (C3SE), provided by the Swedish National Infrastructure for Computing (SNIC).

REFERENCES

[1]N. J. Ashbolt, "Microbial contamination of drinking water and disease outcomes in developing regions," Toxicology **198**, 229–238 (2004).
[2]World Health Organization (WHO) and United Nations Children's Fund (UNICEF), "Progress on drinking water, sanitation and hygiene: 2017 update and SDG baselines," Technical Report (2017), available at https://www.unicef.org/publications/index_96611.html; accessed 8 August 2018.
[3]K. Gopal, S. S. Tripathy, J. L. Bersillon, and S. P. Dubey, "Chlorination byproducts, their toxicodynamics and removal from drinking water," J. Hazard. Mater. **140**, 1–6 (2007).
[4]D. O'Hagan, "Understanding organofluorine chemistry. An introduction to the C-F bond," Chem. Soc. Rev. **37**, 308–319 (2008).
[5]H. Yan, I. T. Cousins, C. Zhang, and Q. Zhou, "Perfluoroalkyl acids in municipal landfill leachates from China: Occurrence, fate during leachate treatment and potential impact on groundwater," Sci. Total Environ. **524-525**, 23–31 (2015).
[6]S. Banzhaf, M. Filipovic, J. Lewis, C. J. Sparrenbom, and R. Barthel, "A review of contamination of surface-, ground-, and drinking water in Sweden by perfluoroalkyl and polyfluoroalkyl substances (PFASs)," Ambio **46**, 335–346 (2017).
[7]K. Berland and P. Hyldgaard, "Exchange functional that tests the robustness of the plasmon description of the van der Waals density functional," Phys. Rev. B **89**, 035412 (2014).
[8]M. Dion, H. Rydberg, E. Schröder, D. C. Langreth, and B. I. Lundqvist, "van der Waals density functional for general geometries," Phys. Rev. Lett. **92**(24), 246401 (2004).
[9]M. Dion, H. Rydberg, E. Schröder, D. C. Langreth, and B. I. Lundqvist, "Erratum: van der Waals density functional for general geometries [Phys. Rev. Lett. 92, 246401 (2004)]," Phys. Rev. Lett. **95**(10), 109902 (2005).
[10]T. Thonhauser, V. R. Cooper, S. Li, A. Puzder, P. Hyldgaard, and D. C. Langreth, "van der Waals density functional: Self-consistent potential and the nature of the van der Waals bond," Phys. Rev. B **76**(12), 125112 (2007).
[11]K. Berland, C. A. Arter, V. R. Cooper, K. Lee, B. I. Lundqvist, E. Schröder, T. Thonhauser, and P. Hyldgaard, "van der Waals density functionals built upon the electron-gas tradition: Facing the challenge of competing interactions," J. Chem. Phys. **140**, 18A539 (2014).
[12]K. Berland, V. R. Cooper, K. Lee, E. Schröder, T. Thonhauser, P. Hyldgaard, and B. I. Lundqvist, "van der Waals forces in density functional theory: A review of the vdW-DF method," Rep. Prog. Phys. **78**, 066501 (2015).
[13]S. D. Chakarova-Käck, E. Schröder, B. I. Lundqvist, and D. C. Langreth, "Application of van der Waals density functional to an extended system: Adsorption of benzene and naphthalene on graphite," Phys. Rev. Lett. **96**(14), 146107 (2006).
[14]S. D. Chakarova-Käck, Ø. Borck, E. Schröder, and B. I. Lundqvist, "Adsorption of phenol on graphite (0001) and α-Al_2O_3 (0001): Nature of van der Waals bonds from first-principles calculations," Phys. Rev. B **74**(15), 155402 (2006).
[15]K. Berland, S. D. Chakarova-Käck, V. R. Cooper, D. C. Langreth, and E. Schröder, "A van der Waals density functional study of adenine on graphene: Single-molecular adsorption and overlayer binding," J. Phys.: Condens. Matter **23**(13), 135001 (2011).
[16]D. Le, A. Kara, E. Schröder, P. Hyldgaard, and T. S. Rahman, "Physisorption of nucleobases on graphene: A comparative van der Waals study," J. Phys.: Condens. Matter **24**(42), 424210 (2012).
[17]J. Åkesson, O. Sundborg, O. Wahlström, and E. Schröder, "A van der Waals density functional study of chloroform and other trihalomethanes on graphene," J. Chem. Phys. **137**(17), 174702 (2012).
[18]E. Schröder, "Methanol adsorption on graphene," J. Nanomater. **2013**, 871706.
[19]J. Ericsson, T. Husmark, C. Mathiesen, B. Sepahvand, Ø. Borck, L. Gunnarsson, P. Lydmark, and E. Schröder, "Involving high school students in computational physics university research: Theory calculations of toluene adsorbed on graphene," PLoS One **11**, e0159168 (2016).
[20]Ø. Borck and E. Schröder, "Methylbenzenes on graphene," Surf. Sci. **664**, 162–167 (2017).
[21]E. Londero, E. K. Karlson, M. Landahl, D. Ostrovskii, J. D. Rydberg, and E. Schröder, "Desorption of n-alkanes from graphene: A van der Waals density functional study," J. Phys.: Condens. Matter **24**(42), 424212 (2012).
[22]E. Kuisma, C. F. Hansson, T. B. Lindberg, C. A. Gillberg, S. Idh, and E. Schröder, "Graphene oxide and adsorption of chloroform: A density functional study," J. Chem. Phys. **144**, 184704 (2016).
[23]T. Ivahnenko and J. S. Zogorski, "Sources and occurrence of chloroform and other trihalomethanes in drinking-water supply wells in the United States, 1986-2001," Technical Report, Scientific Investigations Report 2006-5015, U.S. Department of the Interior and U.S. Geological Survey, 2006.
[24]K. Foxall, "Chloroform toxicological overview," Technical Report, Health Protection Agency, UK, 2007.
[25]J. T. Du, "Toxicological review of chloroform," Technical Report No. 928-CAS No. 67-66-3, U.S. Environmental Protection Agency, Washington, DC, 2001.
[26]Swedish Chemicals Agency, "Hazardous chemicals in textiles—Report of a government assignment, Stockholm," Technical Report No. 3/13 (2013), available at http:www.kemi.se/global/rapporter/2013/rapport-3-13-textiles.pdf; accessed 8 August 2018.
[27]S. Fujii, C. Polprasert, S. Tanaka, N. P. H. Lien, and Y. Qiu, "New POPs in the water environment: Distribution, bioaccumulation and treatment of perfluorinated compounds—A review paper," J. Water Supply: Res. Technol.–AQUA **56**, 313–326 (2007).
[28]M. F. Rahman, S. Peldszus, and W. B. Anderson, "Behavior and fate of perfluoroalkyl and polyfluoroalkyl substances (PFASs) in drinking water treatment: A review," Water Res. **50**, 318–340 (2014).

[29]T. D. Appleman, C. P. Higgins, O. Quiñones, B. J. Vanderford, C. Kolstad, J. C. Zeigler-Holady, and E. R. Dickenson, "Treatment of poly- and perfluoroalkyl substances in U.S. full-scale water treatment systems," Water Res. **51**, 246–255 (2014).
[30]O. Arvaniti and A. Stasinakis, "Review on the occurrence, fate and removal of perfluorinated compounds during wastewater treatment," Sci. Total Environ. **524-525**, 81–92 (2015).
[31]M. Filipovic and U. Berger, "Are perfluoroalkyl acids in waste water treatment plant effluents the result of primary emissions from the technosphere or of environmental recirculation?," Chemosphere **129**, 74–80 (2015).
[32]E. Lutze, S. Panglisch, A. Bergmann, and T. C. Schmidt, "Treatment options for the removal and degradation of polyfluorinated chemicals," in *The Handbook of Environmental Chemistry* (Springer Science and Business Media, 2011), pp. 103–125.
[33]V. A. A. Espana, M. Mallavarapu, and R. Naidu, "Treatment technologies for aqueous perfluorooctanesulfonate (PFOS) and perfluorooctanoate (PFOA): A critical review with an emphasis on field testing," Environ. Technol. Innovation **4**, 168–181 (2015).
[34]A. Lerf, H. He, M. Forster, and J. Klinowski, "Structure of graphite oxide revisited," J. Phys. Chem. B **102**, 4477 (1998).
[35]H.-K. Jeong, Y. P. Lee, R. J. W. E. Lahaye, M.-H. Park, K. H. An, I. J. Kim, C.-W. Yang, C. Y. Park, R. S. Ruoff, and Y. H. Lee, "Evidence of graphitic AB stacking order of graphite oxides," J. Am. Chem. Soc. **130**, 1362–1366 (2008).
[36]T. Thonhauser, S. Zuluaga, C. A. Arter, K. Berland, E. Schröder, and P. Hyldgaard, "Spin signature of nonlocal correlation binding in metal-organic frameworks," Phys. Rev. Lett. **115**, 136402 (2015).
[37]P. Olsson, E. Schröder, P. Hyldgaard, M. Kroon, E. Andreasson, and E. Bergvall, "*Ab initio* and classical atomistic modelling of structure and defects in crystalline orthorhombic polyethylene: Twin boundaries, slip interfaces, and nature of barriers," Polymer **121**, 234 (2017).
[38]P. Olsson, P. Hyldgaard, E. Schröder, E. P. Jutemar, E. Andreasson, and M. Kroon, "*Ab initio* investigation of monoclinic phase stability and martensitic transformation in crystalline polyethylene," Phys. Rev. Mater. **2**, 075602 (2018).
[39]J. Claudot, W. J. Kim, A. Dixit, H. Kim, T. Gould, D. Rocca, and S. Lebègue, "Benchmarking several van der Waals dispersion approaches for the description of intermolecular interactions," J. Chem. Phys. **148**, 064112 (2018).
[40]G. G. Kebede, D. Spångberg, P. D. Mitev, P. Broqvist, and K. Hermansson, "Comparing van der Waals DFT methods for water on NaCl(001) and MgO(001)," J. Chem. Phys. **146**, 064703 (2017).
[41]F. Brown-Altvater, T. Rangel, and J. B. Neaton, "*Ab initio* phonon dispersion in crystalline naphthalene using van der Waals density functionals," Phys. Rev. B **93**, 195206 (2016).
[42]T. Rangel, K. Berland, S. Sharifzadeh, F. Brown-Altvater, K. Lee, P. Hyldgaard, L. Kronik, and J. B. Neaton, "Structural and excited-state properties of oligoacene crystals from first principles," Phys. Rev. B **93**, 115206 (2016).
[43]L. Gharaee, P. Erhart, and P. Hyldgaard, "Finite-temperature properties of nonmagnetic transition metals: Comparison of the performance of constraint-based semilocal and nonlocal functionals," Phys. Rev. B **95**, 085147 (2017).
[44]J. Löfgren, H. Grönbeck, K. Moth-Poulsen, and P. Erhart, "Understanding the phase diagram of self-assembled monolayers of alkanethiolates on gold," J. Phys. Chem. C **120**, 12059 (2016).
[45]Open-source DFT code QE, http://www.quantum-espresso.org/ (2018).
[46]P. Giannozzi, S. Baroni, N. Bonini, M. Calandra, R. Car, C. Cavazzoni, D. Ceresoli, G. L. Chiarotti, M. Cococcioni, I. Dabo, A. D. Corso, S. Fabris, G. Fratesi, S. de Gironcoli, R. Gebauer, U. Gerstmann, C. Gougoussis, A. Kokalj, M. Lazzeri, L. Martin-Samos, N. Marzari, F. Mauri, R. Mazzarello, S. Paolini, A. Pasquarello, L. Paulatto, C. Sbraccia, S. Scandolo, G. Sclauzero, A. P. Seitsonen, A. Smogunov, P. Umari, and R. M. Wentzcovitch, "QUANTUM ESPRESSO: A modular and open-source software project for quantum simulation of materials," J. Phys.: Condens. Matter **21**, 395502 (2009).
[47]G. Román-Pérez and J. M. Soler, "Efficient implementation of a van der Waals density functional: Application to double-wall carbon nanotubes," Phys. Rev. Lett. **103**(9), 096102 (2009).
[48]H. J. Monkhorst and J. D. Pack, "Special points for Brillouin-zone integrations," Phys. Rev. B **13**, 5188 (1976).
[49]J. P. Perdew, K. Burke, and M. Ernzerhof, "Generalized gradient approximation made simple," Phys. Rev. Lett. **77**(18), 3865–3868 (1996).
[50]K. Garrity, J. Bennett, K. Rabe, and D. Vanderbilt, "Pseudopotentials for high-throughput DFT calculations," Comput. Mater. Sci. **81**, 446 (2014).
[51]By position, we here mean which parts of GO are overlapped by the adsorbed molecule, not how the parts of the molecule are oriented within that position.
[52]With one exception: Orientation 1 for PFHxS on GO has a smaller adsorption energy (991 meV) than both the shorter PFBS (1062 meV) and the longer PFOS (1214 meV).
[53]Y. Jiao, E. Schröder, and P. Hyldgaard, "Signatures of van der Waals binding: A coupling-constant scaling analysis," Phys. Rev. B **97**, 085115 (2018).
[54]P. Hyldgaard, K. Berland, and E. Schröder, "Interpretation of van der Waals density functionals," Phys. Rev. B **90**(7), 075148 (2014).
[55]T. Steiner, "The hydrogen bond in the solid state," Angew. Chem., Int. Ed. **41**, 48–76 (2002).
[56]J. Klimeš, D. R. Bowler, and A. Michaelides, "Chemical accuracy for the van der Waals density functional," J. Phys.: Condens. Matter **22**, 022201 (2010).
[57]P. Jurecka, J. Sponer, J. Cerny, and P. Hobza, "Benchmark database of accurate (MP2 and CCSD(T) complete basis set limit) interaction energies of small model complexes, DNA base pairs, and amino acid pairs," Phys. Chem. Chem. Phys. **8**(17), 1985–1993 (2006).
[58]E. Schröder, Preliminary results of PAH molecules on graphene, compared with desorption experiments presented in Ref. 59.
[59]R. Zacharia, H. Ulbricht, and T. Hertel, "Interlayer cohesive energy of graphite from thermal desorption of polyaromatic hydrocarbons," Phys. Rev. B **69**, 155406 (2004).